REFERENCES
Adler, A. J., Hoving, R., Potter, J., Wells, M., & Fasman, G. D., (1968) *J. Am. Chem. Soc. 90*, 4736–4741.
Aebersold, D., & Pysh, E. S. (1970) *J. Chem. Phys. 53*, 2156–2163.
Bramson, H. N., Kaiser, E. T., & Mildvan, A. S. (1984) *CRC Crit. Rev. Biochem. 15*, 93–124.
Cleland, W. W. (1967) *Adv. Enzymol. Relat. Areas Mol. Biol. 29*, 1–32.
Cook, D. F., Neville, M. E., Vrana, K. E., Hartl, F. T., & Roskoski, R. R. (1982) *Biochemistry 21*, 5794–5799.
Daile, P., Carnegie, P. R., & Young, J. K. (1975) *Nature (London) 257*, 416–418.
Feramisco, J. R., Glass, D. B., & Krebs, E. G. (1979) *J. Biol. Chem. 255*, 4240–4245.
Granot, J., Mildvan, A. S., Bramson, H. N., Thomas, N., & Kaiser, E. T. (1981) *Biochemistry 20*, 602–610.
Greenfield, N. J., & Fasman, G. D. (1969) *Biochemistry 8*, 4180–4186.
Kemp, B. E. (1979) *J. Biol. Chem. 254*, 2638–2642.
Kemp, B. E., Graves, D. J., Benjamini, E., & Krebs, E. G. (1977) *J. Biol. Chem. 252*, 4888–4894.
Kübler, D., Gagelmann, M., Pyerin, W., & Kinzel, V. (1979) *Hoppe-Seyler's Z. Physiol. Chem. 360*, 1421–1423.
Matsuo, M., Huang, C.-H., & Huang, L. (1980) *Biochem. J. 187*, 371–379.
Meggio, F., Chessa, G., Borin, G., Pinna, L. A., & Marchiori, F. (1981) *Biochim. Biophys. Acta 662*, 94–101.
Provencher, S. W., & Glockner, J. (1981) *Biochemistry 20*, 33–37.
Reed, J., & Kinzel, V. (1984a) *Biochemistry 23*, 968–973.
Reed, J., & Kinzel, V. (1984b) *Biochemistry 23*, 1357–1362.
Reed, J., Gagelmann, M., & Kinzel, V. (1983) *Arch. Biochem. Biophys. 222*, 276–284.
Whitehouse, S., & Walsh, D. A. (1983) *J. Biol. Chem. 258*, 3682–3692.
Whitehouse, S., Feramisco, J. R., Casnellie, J. E., Krebs, E. G., & Walsh, D. A. (1983) *J. Biol. Chem. 258*, 3693–3701.
Witt, J. J., & Roskoski, R. (1975) *Biochemistry 14*, 4503–4507.
Zetterquist, O., Ragnarsson, U., Humble, E., Berglund, L., & Engstrom, L. (1976) *Biochem. Biophys. Res. Commun. 76*, 696–703.

Hydrogen Exchange Kinetics of Core Peptide Protons in *Streptomyces* Subtilisin Inhibitor†

Kazuyuki Akasaka,* Tomoko Inoue, Hiroyuki Hatano, and Clare K. Woodward

Department of Chemistry, Faculty of Science, Kyoto University, Kyoto 606, Japan, and Department of Biochemistry, The University of Minnesota, St. Paul, Minnesota 55108

Received July 6, 1984; Revised Manuscript Received December 6, 1984

ABSTRACT: The hydrogen isotope exchange kinetics of the 10 slowest exchanging resonances in the ^{1}H NMR spectrum of *Streptomyces* subtilisin inhibitor (SSI) have been determined at pH 7–11 and 30–60 °C. These resonances are assigned to peptide amide protons in the β-sheet core that comprises the extensive protein–protein interface of the tightly bound SSI dimer. The core protons are atypical in that their exchange rates are orders of magnitude slower than those for all other SSI protons. When they do exchange at temperatures >50 °C, they do so as a set and with a very high temperature coefficient. The pH dependence of the exchange rate constants is also atypical. Exchange rates are approximately first order in hydroxyl ion dependence at pH <8.5 and >9.5 and pH independent between pH 8.5 and 9.5. The pH dependence and temperature dependence of the SSI proton exchange rates are interpreted by the two-process model [Woodward, C. K., & Hilton, B. D. (1980) *Biophys. J. 32*, 561–575]. The results suggest that in the average solution structure of SSI, an unusual mobility of secondary structural elements at the protein surface is, in a sense, compensated by an unusual rigidity and inaccessibility of the β-sheet core at the dimer interface.

Streptomyces subtilisin inhibitor (SSI) inhibits alkaline proteases of bacterial origin (Sato & Murao, 1973). In its native form, SSI is an elongated dimer composed of two identical polypeptides, each containing 113 amino acids and 2 disulfide bonds (Ikenaka et al., 1974). The secondary structure of the monomer consists of a five-stranded β-sheet and two short α-helices, and the dimer interface involves extensive contacts between β-sheet strands of the monomers (Mitsui et al., 1979). The accessible area buried upon dimerization is 786 Å^2 per monomer, 12.7% of the total static solvent-accessible surface area of dissociated (hypothetical) monomer (Satow et al., 1980). In neutral aqueous solution, SSI dimer is tightly bound with a dissociation constant on the order of 10^{-13} M (Akasaka et al., 1982a). SSI has a p*I* of 4.3 (Sato & Murao, 1974) and is unusually stable against thermal and alkaline denaturation (Akasaka et al., 1982b,c; Takahashi & Sturtevant, 1981; Fujii et al., 1981; Akasaka, 1978). SSI has two regions of exposed peptide segments per subunit, residues 1–7 and 64–75. The latter carries the binding loop for proteases (Hirono et al., 1979). Increased mobility of the exposed peptide segments relative to the rest of the protein

†C.K.W. was supported by National Institutes of Health Grant GM26242.

* Address correspondence to this author at the Department of Chemistry, Kyoto University.

0006-2960/85/0424-2973$01.50/0

is indicated by the disorder in part of these segments in the X-ray structure (Mitsui et al., 1979) and by the differential efficiency of spin diffusion in ^1H NMR cross-saturation experiments (Akasaka, 1983).

In the present work, we have characterized the hydrogen exchange kinetics of a group of protons that exchange qualitatively slower than the other SSI NH's. This group is assigned to the β-sheet region of the protein, which we refer to as the β-core. Their exchange properties differ from any reported in other proteins. Generally, while the NH's in native proteins exchange with a spread of first-order rates that ranges over 6–10 orders of magnitude, the distribution is fairly continuous. The exchange rates for the β-core protons in SSI, however, do not overlap with the distribution of rates of the other SSI NH's. Further, at pH <9, these protons apparently exchange only at high temperatures by a mechanism involving major disruption of the protein. The data indicate that SSI has a β-core that is extraordinarily rigid and inaccessible to solvent. This is particularly interesting since the β-core region is at the dimer interface and since most of the NH's in the rest of SSI exchange unusually rapidly. The dynamic structure of SSI that emerges is one of a highly mobile surface organized around a very rigid β-sheet composing the protein–protein interface.

Materials and Methods

Crude lyophilized SSI, kindly supplied by Professor Murao of Osaka Prefectural University, was further purified by the method of Sato & Murao (1973). Prior to the hydrogen exchange measurements, purified, lyophilized SSI was dissolved in ^2H_2O, adjusted to pH 9 with NaO^2H, and incubated at 45 °C for 12–18 h to deuterate the rapidly exchanging protons. An aliquot of the solution was mixed with an equal volume of deuterated buffer to give a final concentration of 36–75 mg/mL SSI, 0.1 M NaCl, and 0.1 M buffer. The pH of the sample was checked before and after the exchange experiment. Buffers used were sodium phosphate at pH 7–8 and pH 11, sodium borate at pH 8–10, and sodium carbonate at pH 10–11.

The ^1H NMR spectra were measured on a Nicolet NT spectrometer operating at 300 MHz using 5-mm-diameter tubes. A 45° sampling pulse with a total repetition of 1 s, or a 90° pulse with a total repetition of 2 s, was applied. The free induction decay signals were accumulated over 100–1000 scans. The probe temperature, regulated to ±1 °C, was monitored by the chemical shift of the hydroxy proton of ethylene glycol (sample and shift-temperature conversion tables were supplied by Varian Associates).

pH values are the direct readings of a pH meter standardized against H_2O buffers. Chemical shifts are given relative to the methyl peak of sodium (trimethylsilyl)propionate-*2,2,3,3-d*$_4$.

Results

The downfield region of the ^1H NMR spectrum of SSI in Figure 1 contains 34 nonexchangeable resonances assigned to the aromatic ring protons of 3 tyrosine, 1 tryptophan, 3 phenylalanine, and 2 histidine residues in the envelope at 6.4–7.6 ppm (Fujii et al., 1981; Akasaka et al., 1975) and 2 C-2 imidazole protons assigned to His-43 and His-106 at 7.9 and 8.1 ppm, respectively (Fujii et al., 1980). The exchangeable resonances downfield of the histidine C-2 peaks are assigned to peptide NH's (Akasaka et al., 1975), of which there are 104 in SSI. There is one tryptophan residue, Trp-86; its indole NH has an exchange rate constant of 10 s^{-1} at 25 °C, pH 8.1 (Takahashi et al., 1978; Tsuboi, 1982), and is too rapidly

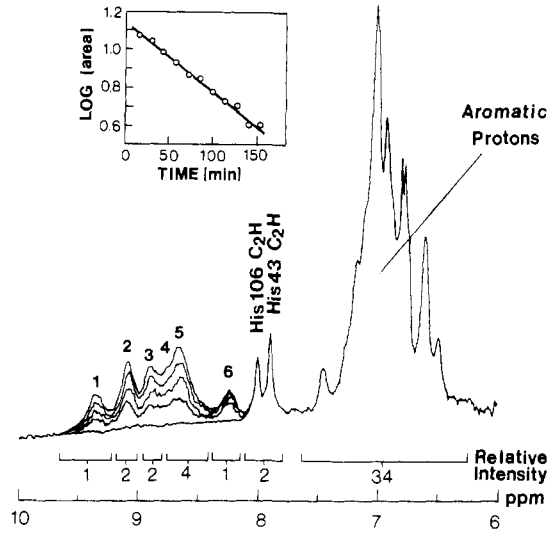

FIGURE 1: Low-field region of the 300-MHz ^1H NMR spectrum of SSI after incubation for 12 h at 45 °C, pH 9. The sample contains 72 mg of SSI per milliliter of deuterated borate buffer at 0.1 M NaCl. The four upper spectra in the region 8.4–9.7 ppm were recorded at 54 °C, pH 9, after 14, 44, 89, and 180 min at 54 °C. The base-line spectrum in that region was recorded after 60 min at 63 °C. Peptide NH resonances are numbered above the spectra. Peak intensities, determined relative to the 34 nonexchangeable aromatic protons at 45 °C, are given below the spectra. From the slope of the semilogarithmic plot of the total area of peaks 1–5 against time of incubation at 54 °C (inset), the apparent exchange rate constant is 6.5×10^{-3} min^{-1}.

exchanging to be seen in these experiments.

Most of the NH's in SSI exchange with deuterium within 1 h after the protein is dissolved in ^2H_2O at room temperature around neutral pH. At 27 °C pH 9, there is an exchangeable ^1H intensity equivalent to 18 protons in the region 7.5–10 ppm after 1 h in ^2H_2O. Eight of these exchange with measurable rates as the temperature is raised to 40 °C. The remaining intensity of 10 protons does not change after several days at 45 °C, pH 9. We refer to this exceptionally slowly exchanging group as the SSI core peptide protons. Their ^1H NMR resonances are observed at 8.15–9.6 ppm in spectra of SSI that has been preincubated at pH 9, 45 °C overnight (Figure 1). Their ^1H–^2H exchange rates are determined from the decay with time in deuterium solvent of the ^1H intensity of peaks 1, 2, 3, 5, and 6 at 9.4, 9.1, 8.9, 8.65, and 8.25 ppm, respectively (Figure 1). Peak 4 at 8.8 ppm appears only as a shoulder of peak 5, and its intensity cannot be measured separately.

Peak 1 has an intensity of 1, and its exchange follows a first-order rate law. Each of peaks 2 and 3 has an intensity of ~2, and peaks 4 and 5 have a combined intensity of ~4. The rate constants determined from the decay intensity of peaks 2, 3, and 5 are, then, an average of the component resonances. However, under all conditions measured, peaks 2–5 have first-order exchange rate constants. The exchange rate constants obtained from the heights of peaks 1–5 and the rate constant obtained from the decay of total area under the spectrum between 8.4 and 9.7 ppm (Figure 1 inset) are the same within a factor of 1.3 at pH 7–9. The exchange of peak 6 is first order, but its rate is slower than for peaks 1–5.

The SSI core peptide protons have several remarkable exchange characteristics. First, they exchange qualitatively slower than all the other NH's in the protein. Second, they exchange as a group at temperatures >50 °C, pH 7–9. Third, their exchange rates are highly temperature dependent; at 45 °C, pH 9, no exchange is measured after several days, while at 60 °C, pH 9, their exchange is at the fast limit for this

Table I: Hydrogen Exchange Rate Constants for SSI Core Protons[a]

pH	temp (°C)	k_{obsd} (min^{-1}) for peak 1	2	3	5	6
7.0	56	1.72×10^{-3}	1.40×10^{-3}	1.97×10^{-3}	1.90×10^{-3}	
7.1	56	1.05×10^{-3}	1.09×10^{-3}	1.33×10^{-3}	1.07×10^{-3}	
	58.5	4.93×10^{-3}	3.97×10^{-3}	4.35×10^{-3}	3.12×10^{-3}	
	60.5	8.63×10^{-3}	8.70×10^{-3}	1.00×10^{-2}	8.28×10^{-3}	2.99×10^{-3}
	62.5	1.62×10^{-2}	1.39×10^{-2}	2.18×10^{-2}	1.64×10^{-2}	3.32×10^{-3}
	64.5	2.36×10^{-2}	2.22×10^{-2}	3.44×10^{-2}	2.21×10^{-2}	
	66	6.99×10^{-2}	7.61×10^{-2}	1.03×10^{-1}	8.44×10^{-2}	2.87×10^{-2}
7.5	54	1.08×10^{-3}	0.89×10^{-3}	1.02×10^{-3}	1.02×10^{-3}	
	56	3.13×10^{-3}	2.75×10^{-3}	3.66×10^{-3}	3.42×10^{-3}	
7.9	54	3.04×10^{-3}	2.16×10^{-3}	2.11×10^{-3}	2.13×10^{-3}	
8.1	56	6.19×10^{-3}	5.98×10^{-3}	7.86×10^{-3}	6.86×10^{-3}	2.21×10^{-3}
8.5	56	1.28×10^{-3}	1.18×10^{-2}	1.25×10^{-2}	1.04×10^{-2}	
8.7	56	$\gtrsim 1.0 \times 10^{-2}$	1.13×10^{-2}	$\gtrsim 1.0 \times 10^{-2}$	1.17×10^{-2}	
8.8	54	5.78×10^{-3}	5.84×10^{-3}	6.46×10^{-3}	7.06×10^{-3}	
9.0	50.5	1.79×10^{-3}	1.63×10^{-3}	1.99×10^{-3}	2.53×10^{-3}	
	54	6.76×10^{-3}	5.39×10^{-3}	6.15×10^{-3}	6.67×10^{-3}	3.08×10^{-3}
	56	1.20×10^{-2}	1.00×10^{-2}	1.10×10^{-2}	1.27×10^{-2}	6.77×10^{-3}
	57.5	2.45×10^{-2}	1.62×10^{-2}	2.02×10^{-2}	1.94×10^{-2}	7.73×10^{-3}
	58.5	2.63×10^{-2}	2.55×10^{-2}	2.97×10^{-2}	2.55×10^{-2}	1.55×10^{-2}
	60.5	4.46×10^{-2}	4.73×10^{-2}	4.81×10^{-2}	4.34×10^{-2}	2.60×10^{-2}
	62.5	9.49×10^{-2}	9.76×10^{-2}	1.04×10^{-1}	1.09×10^{-1}	6.72×10^{-2}
9.2	54	6.53×10^{-3}	4.88×10^{-3}	5.15×10^{-3}	6.58×10^{-3}	
	56	8.87×10^{-3}	9.93×10^{-3}	9.59×10^{-3}	1.03×10^{-2}	
9.5	56	1.70×10^{-2}	1.75×10^{-2}	2.00×10^{-2}	2.13×10^{-2}	1.04×10^{-2}
9.7	56	1.98×10^{-2}	1.80×10^{-2}	1.86×10^{-2}	2.61×10^{-2}	
10.0	54	9.38×10^{-3}	7.02×10^{-3}	7.95×10^{-3}	1.05×10^{-2}	6.46×10^{-3}
	56	3.36×10^{-2}	2.46×10^{-2}	3.07×10^{-2}	3.43×10^{-2}	1.69×10^{-2}
10.1	56	4.46×10^{-2}	2.52×10^{-2}	4.20×10^{-2}	5.82×10^{-2}	
10.2	56	3.50×10^{-2}	2.34×10^{-2}	3.11×10^{-2}	4.30×10^{-2}	
10.3	56	$\gtrsim 3.0 \times 10^{-2}$	3.06×10^{-2}	3.26×10^{-2}	$\gtrsim 3.5 \times 10^{-2}$	
10.5	46.5	2.96×10^{-3}	1.24×10^{-3}	1.53×10^{-3}	4.22×10^{-3}	
	48.5	7.62×10^{-3}	3.02×10^{-3}	3.46×10^{-3}	8.48×10^{-3}	4.49×10^{-3}
	51.5	$\gtrsim 2.0 \times 10^{-2}$	1.21×10^{-2}	8.74×10^{-3}	$\gtrsim 2.0 \times 10^{-2}$	
	54	$\gtrsim 2.0 \times 10^{-2}$	2.22×10^{-2}	2.29×10^{-2}	2.89×10^{-2}	1.89×10^{-2}
	56	4.16×10^{-2}	2.32×10^{-2}	2.29×10^{-2}	3.84×10^{-2}	2.00×10^{-2}
	57.5	5.74×10^{-2}	3.84×10^{-2}	4.49×10^{-2}	5.73×10^{-2}	3.36×10^{-2}
11	54	$\gtrsim 6.0 \times 10^{-2}$	5.49×10^{-2}	5.82×10^{-2}	$\gtrsim 6.0 \times 10^{-2}$	

[a] The hydrogen exchange rate constants were determined by a least-squares fit of a first-order rate equation to experimental peak height vs. time of peaks 1, 2, 3, and 5 measured at 9.4, 9.1, 8.9, and 8.65 ppm, respectively.

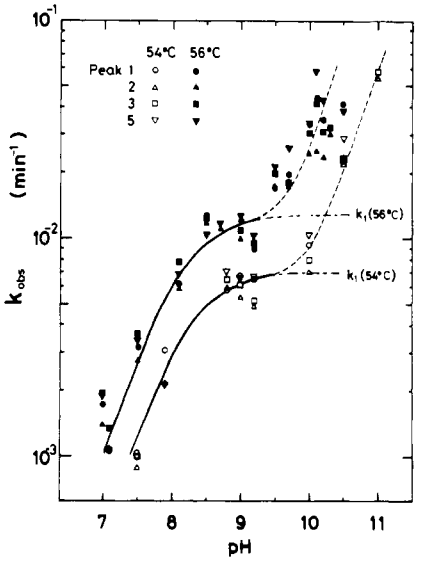

FIGURE 2: pH dependence of the exchange rate constants of SSI core protons at 54 °C (open symbols) and at 56 °C (closed symbols). The solid lines are calculated from eq 2 as described in the text.

method. Fourth, the SSI core peptide protons display an unusual variation with pH in the range pH 7–11.

The pH dependence of the exchange of peaks 1–5 is shown in Figure 2. At pH <8.5 and >10, the exchange rate increases logarithmically with pH, corresponding to the well-known base

Table II: Apparent Activation Energies for Hydrogen Exchange Rate Constants of SSI Core Protons at pH 7.1, 9.0, and 10.5

pH	$\Delta H^{\ddagger}$ (kcal/mol)[a] for peak 1	2	3	5	6
7.1	83.4 ± 7.7	84.7 ± 7.5	90.6 ± 4.9	89.3 ± 7.4	
9.0	69.5 ± 2.9	73.0 ± 1.5	70.6 ± 1.8	65.2 ± 2.7	71.2 ± 3.0
10.5	53.7 ± 4.6	63.5 ± 7.5	61.9 ± 4.9	47.7 ± 2.4	56.5 ± 7.3

[a] Activation energies and standard deviations were calculated from a linear regression analysis of the data in Table I.

catalysis of the NH chemical exchange step. However, in the range pH 8.5–9.5, the exchange rate constants are relatively pH independent.

This type of pH dependence has been reported for two other slowly exchanging protons, the peptide NH's of Tyr-21 and Phe-22 of bovine pancreatic trypsin inhibitor (BPTI). These are the slowest exchanging NH's among a group of very slowly exchanging peptide protons H bonded in the β-sheet of BPTI. The pH independence of BPTI Tyr-21 and Phe-22 in the range pH 8.4–9.6 has been interpreted as a switch in exchange mechanism in this pH range from a process involving major cooperative unfolding to one involving fluctuations of the folded state (Woodward & Hilton, 1980; Hilton et al., 1981; Woodward et al., 1982). These two processes are distinguished by their temperature coefficients. The process involving major unfolding has a higher apparent activation energy ($\Delta H^{\ddagger}$), reflecting the enthalpy of unfolding, and the process involving fluctuations of the folded state has a lower $\Delta H^{\ddagger}$, which for

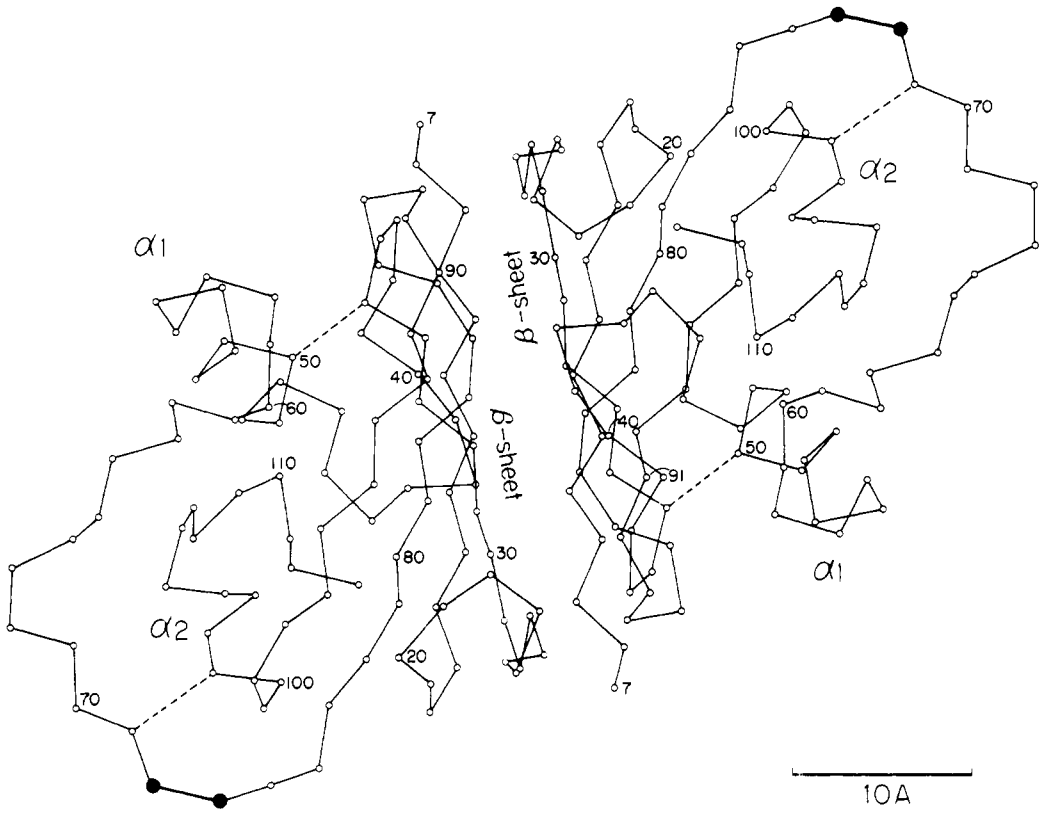

FIGURE 3: Crystal structure of SSI, represented by the α-carbon backbone (—) and disulfide bridges (---) (Mitsui et al., 1979). The diad axis relating the two identical subunits lies perpendicular to the paper. The six N-terminal residues are missing from the figure, as they give no electron density. The subunit interface is comprised of a 5-fold antiparallel β-sheet, with strands of opposite subunits mutually inclined by about 30°. The molecular dimensions for the dimer are 30 × 40 × 65 Å^3.

most proteins is in the range 20–35 kcal/mol (84–146 kJ/mol).

To test the applicability of the two-process model to the SSI core proton exchange mechanism, the temperature dependence of the exchange rate constants at pHs above, below, and in the middle of the pH-independent region was determined. The rate constants at pH 7–11 are given in Table I. The activation energies at pH 7.1, 9, and 10.5 are given in Table II.

Although the temperature range over which the rate constants can be measured is limited, the trend is clear. At pH 7, $\Delta H^{\ddagger} \simeq 87$ kcal/mol (364 kJ/mol); at pH 9, $\Delta H^{\ddagger} \simeq 70$ kcal/mol (293 kJ/mol); and at pH 10.5, $\Delta H^{\ddagger}$ varies between 48 and 64 kcal/mol (201–268 kJ/mol).

The rate constant of peak 6 is about one-third that of peaks 1–5. However, its pH and temperature dependence is the same as for peaks 1–5, strongly suggesting that it also arises from the β-core. Its slower exhange rate could arise from local effects on the chemical exchange step.

Discussion

In the SSI crystal structure, 56 of the 104 exchangeable peptide NH's per monomer have static accessibilities of zero (Satow et al., 1980). Only about 30% of the 56 buried NH's exchange slowly enough at pH >7 to be measured by this technique, 8 with measurable exchange rate constants at 25–45 °C, pH 9, and the 10 remaining core protons with exchange rates measurable only at temperatures >50 °C. This division of SSI exchangeable protons into well-separated kinetic classes was also reported by Nakanishi & Tsuboi (1976) from experiments using infrared absorption. They classified the exchangeable protons of SSI into three groups: 72 fast, 15 intermediate, and 17 slow NH's. The number of protons in the last group corresponds well with the number we find remaining unexchanged at 27 °C, pH 9.

In this paper, we consider the 10 slowest exchanging core protons. It is likely that these are core peptide NH's H bonded in the β-sheet region of the dimer interface.[1] The SSI crystal structure (Figure 3) has 5 strands of β-sheet per monomer containing 24 H-bonded peptide NH's and 2 strands of α-helix containing 13 H-bonded NH's (Satow et al., 1980). The dimer interface is formed by three strands of β-sheet from each monomer with extensive intermolecular contacts (Satow et al., 1980). The protein–protein contacts are essentially nonpolar; there are only three H bonds possible between monomers, and these involve side chains. The slowest exchanging NH's in other proteins which have been assigned are typically found in the β-sheet (Dubs et al., 1979; Kossikoff, 1982).

The SSI core protons are selectively labeled with ^{1}H by incubation of the protein in deuterium at 45 °C, pH 9. Their pH and temperature dependence may be analyzed by the "two-process" model proposed for the slowest exchanging BPTI NH's (Woodward & Hilton, 1980; Hilton et al., 1981). In

[1] There is preliminary evidence that the slowest exchanging NH's studied here are in the β-sheet. In separate NOE experiments, peaks 1 and 2 were selectively saturated by continuous radio-frequency irradiation. The saturation is transferred efficiently to resonances at 4.3 and 5.6 ppm, respectively, which are assigned to $C_\alpha H$ protons. Such an efficient transfer of saturation is usually found only in the β-sheet where the $C_\alpha H$–NH distance of two successive residues in the sequence is small, ~2.2 Å (Dubs et al., 1979). From the initial growth rate of the NOE difference and the rotational correlation time of the protein, the $C_\alpha H$–NH distance may be calculated (Dubs et al., 1979). Using a rotational correlation time of 10^{-8} s (Abe et al., 1979), we computed a $C_\alpha H$–NH distance of <2.6 Å for these protons, less than the distance usually found in an α-helix, ≥2.9 Å (Dubs et al., 1979). Similar experiments with peaks 3–6 are not feasible because of the overlap of the HO^{2}H resonance. In addition, the exchange rate of an NH assigned to a β-sheet residue is comparable to the exchange rates of the core protons reported here (M. Kainosho, private communication).

Table III: Equilibrium Constants for the Cooperative Unfolding/Folding Transition of SSI Determined from Hydrogen Exchange Rate Constants at pH 7.1, 55–66 °C, with Associated Enthalpy and Entropy of Denaturation

parameter	K_{eq}[a] for peak 1	2	3	5	
temp (°C)					
56	1.09×10^{-7}	1.14×10^{-7}	1.39×10^{-7}	1.11×10^{-7}	
58.5	4.18×10^{-7}	3.36×10^{-7}	3.69×10^{-7}	2.64×10^{-7}	
60.5	6.25×10^{-7}	6.30×10^{-7}	7.26×10^{-7}	6.00×10^{-7}	
62.5	1.00×10^{-6}	8.58×10^{-7}	1.35×10^{-6}	1.01×10^{-6}	
64.5	1.25×10^{-6}	1.17×10^{-6}	1.82×10^{-6}	1.17×10^{-6}	
66	3.28×10^{-6}	3.57×10^{-6}	4.83×10^{-6}	3.96×10^{-6}	
$\Delta H°$ (kcal/mol)	65.8 ± 7.7	67.0 ± 7.5	73.0 ± 4.9	71.8 ± 7.4	69.4[b]
$\Delta S°$ [cal/(deg·mol)]	169 ± 23	172 ± 22	191 ± 15	187 ± 22	180[b]

[a] K_{eq} is obtained by dividing k_{obsd} by k_{cx}, where $k_{cx} = 60 \times 6.4 \times 10^{6+pH-3850/T}$ min^{-1} with T the absolute temperature (Takashashi et al., 1978). [b] Average value.

this model, the observed rate constant of proton i, $k_{obsd,i}$ is the sum of its exchange by two pathways:

$$k_{obsd,i} = k_{l,i} + k_{h,i} \quad (1)$$

where $k_{l,i}$ is the rate constant for the lower activation energy exchange process involving local fluctuations of the protein and $k_{h,i}$ is the rate constant for the higher activation energy process of exchange involving global unfolding. When $k_{h,i} >> k_{l,i}$, as may be the case for the slowest exchanging protons at lower pH, then $k_{obsd,i} = k_{h,i}$, and proton i exchanges by the major unfolding pathway. When $k_{h,i} << k_{l,i}$, as may be the case at higher pH when the base-catalyzed k_{cx} is larger, proton i exchanges by the pathway involving more localized motions.

Generally, k_l is proportional to the exchange rate constant for the chemical exchange step of free peptides, k_{cx}, which shows first-order base catalysis at pH >4. The expression for k_h includes the overall rate constant of unfolding in the cooperative denaturation transition, k_1, and the rate constant for refolding, k_2:

$$k_h = k_l k_{cx}/(k_1 + k_2 + k_{cx}) \quad (2)$$

Under conditions that favor the native conformation, $k_1 << k_2$, and when $k_{cx} << k_2$

$$k_h \simeq k_l k_{cx}/k_2 \simeq K_{eq} k_{cx} \quad (3)$$

where K_{eq} is the equilibrium constant for cooperative unfolding (Woodward & Hilton, 1979). When $k_{cx} >> k_1$

$$k_h \simeq k_1 \quad (4)$$

In the two-process explanation of the data in Figure 2, $k_{h,i} >> k_{l,i}$ at pH 7–9.5, and eq 2–4 apply, but at pH >9.5, $k_{l,i} >> k_{h,i}$. At pH 7–8.5, the observed change rate constant is approximated by the right side of eq 3. In the pH-independent region, pH 8.5–9.5, the unfolding rate is slow relative to the chemical exchange rate k_{cx}, and k_1 becomes rate limiting (eq 4). At pH >9.5, the observed exchange of proton i is dominated by $k_{l,i}$ which is proportional to the base-catalyzed k_{cx} and which at high pH becomes larger than k_1.

This explanation predicts several properties of the temperature dependence of the SSI core protons at pH 7, 9, and 10.5. First, at pH 7, the exchange rate constants and activation energies should be approximately the same for all core NH's, since $k_{h,i} >> k_{l,i}$ and exchange is governed by the same process, major unfolding. Further, the value of $\Delta H°$ for the reversible denaturation of SSI derived at pH 7 by application of eq 3 should be comparable to the $\Delta H°$ obtained from independent experiments. In addition, the variation with pH of the rate constant for exchange calculated from eq 2 should agree with observed rates in the range pH 7–9. Second, at pH 9, the exchange rate constants and activation energies should be the same for all core protons, and the value of the activation energy of the exchange rate constant should equal the activation energy of k_1 (eq 4). Third, at pH 10.5, the exchange rate constants and their activation energies should be different from each other since the low activation energy mechanism will probably differ for each proton. The data in Tables II and III are consistent with each of these.

In the pH range 7–8.5, K_{eq} can be estimated from eq 3 when k_{cx} is known. A value for k_{cx} can be obtained from the empirical expression determined for poly(DL-alanine) at pH 5–8 in 50:50 $^1H_2O/^2H_2O$

$$k_{cx} = 60 \times 6.4 \times 10^{6+pH-3850/T} \text{ min}^{-1} \quad (5)$$

where the temperature (T) is in degrees kelvin (Takahashi et al., 1978). The values for K_{eq} at pH 7 calculated from eq 3 as a function of temperature are given in Table III. The $\Delta H°$ values obtained from peaks 1–5 at pH 7 agree with each other within experimental error, as do the $\Delta S°$ values.

The variation with pH of the rate constant for exchange by the high activation energy process over the range pH 7–9.2 can be calculated from eq 2. Using k_{cx} determined from eq 5 and the value of K_{eq} determined as described above, and assuming k_1 and k_2 to be pH independent, we fit the experimental points in Figure 2 to eq 2 to yield the most probable value of k_1. At 54 °C $k_1 = 7.1 \times 10^{-3}$ min^{-1}, and at 56 °C $k_1 = 1.3 \times 10^{-2}$ min^{-1}. The calculated curves are shown by full lines in Figure 2, and the good fit supports the suggestion that exchange at pH 7–9 is via cooperative unfolding.

The $\Delta H°$ value determined by applying eq 3 to the data at pH 7, 56–66 °C, is ~70 kcal/mol (~293 kJ/mol) (Table III). The calorimetrically determined enthalpy of denaturation, ΔH_d, is considerably higher. At the transition temperature, 83 °C, ΔH_d = 122.2 kcal/mol for SSI (dimer) (Takahashi & Sturtevant, 1981). However, there is a heat capacity difference between the native and the denatured proteins ($\Delta C_p \neq 0$), and the enthalpy and the entropy of denaturation are temperature dependent. Extrapolation of the thermodynamic parameters to lower temperature may be made with the relations:

$$\Delta H(T) = \Delta H_d - \Delta C_{p,d}(T_d - T) \quad (6)$$

$$\Delta S(T) = \Delta H_d/T_d - \Delta C_{p,d} \ln (T_d/T) \quad (7)$$

$$\Delta G(T) = \Delta H(T) - T\Delta S(T) \quad (8)$$

assuming that ΔC_p is constant over the temperature range of extrapolation and therefore may be set equal to $\Delta C_{p,d}$, the heat capacity difference between the denatured and the native proteins at T_d (Privalov & Khechinashivili, 1974). H_d is the standard enthalpy of the unfolding at the denaturation temperature, T_d.

The extrapolated thermodynamic quantities are expected to give approximate values at temperatures not too far from

T_d (Lapanje, 1978). In ^2H_2O, T_d is higher than in ^1H_2O by ~5 °C (Nakanishi & Tsuboi, 1976; Komiyama et al., 1984). The thermodynamic quantities predicted from eq 6–8 for the temperature range 51–61 °C in ^1H_2O, rather than those for 56–66 °C, should be compared with those obtained from the ^1H–^2H exchange study for 56–66 °C in ^2H_2O. Putting the above ΔH_d and T_d values together with a $\Delta C_{p,d}$ of 1.097 kcal mol^{-1} K^{-1} (4.59 kJ/mol) (Takahashi & Sturtevant, 1981), we obtain

$$\Delta H = 92.4 \pm 5.5 \text{ kcal mol}^{-1}$$

$$\Delta S = 0.257 \pm 0.017 \text{ kcal mol}^{-1} \text{ K}^{-1}$$

$$\Delta G = 7.9 \pm 1.3 \text{ kcal mol}^{-1}$$

for thermodynamic quantities extrapolated to 56 ± 5 °C.

These values are fairly close to $\Delta H°$ = 70 kcal/mol (293 kJ/mol), $\Delta S°$ = 0.180 kcal mol^{-1} K^{-1} (0.753 kJ/mol), and $\Delta G°$ = 9.5 kcal/mol (39.7 kJ/mol) determined above from the ^1H–^2H exchange study at 56–66 °C in ^2H_2O. This supports the suggestion that the conformational transition monitored by the ^1H–^2H exchange of the core protons at pH 7–9 is of major cooperative unfolding.

In the two-process model, exchange in the pH-independent region around pH 9 is given by eq 4, and the observed $\Delta H^‡$ for exchange, 70 kcal/mol (293 kJ/mol) (Table II), is the activation energy of k_1. The $\Delta H^‡$ of k^1 for the SSI denaturation transition has not been determined, but in other proteins, the activation energy of k_2 is small, and $\Delta H°$ is approximately equal to the activation energy of k_1 (Pohl, 1968; Segawa et al., 1973). The activation energy of the exchange rate constant at pH 9 is within error of $\Delta H°$ determined from the exchange data at pH 7 (Table III).

If exchange at pH <9.4 involves the cooperative unfolding transition, then the exchange rates in this range should be faster for SSI derivatives that are more thermally labile.[2] This has been observed for SSI*, in which the reactive peptide bond, Met-73–Val-74, has been hydrolyzed with concomitant loss of the six N-terminal residues in the 74–113 fragment (Matsumori et al., 1982). The cleaved scissile bond is located in the exposed arm of the molecule, >20 Å from the β-sheet dimer interface. SSI* retains a folded, active conformation, but its denaturation midpoint temperature is >10 °C lower than the parent SSI. A set of 10 slowly exchanging NH's is observed in the SSI* NMR spectrum at pH 9, and they exchange as a group, but at lower temperature than in SSI. The time constant for the exchange of the SSI* core protons at pH 9, 45 °C, is the same as for the SSI core protons at pH 9, 56 °C (Akasaka et al., 1983).

Implicit in a two-process analysis of the SSI data are the assumptions that, over the pH and temperature range studied, exchange takes place from the dimeric complex and k_1 is pH independent. The available data indicate that these are reasonable assumptions. The SSI dimer is so tightly associated that the dissociation constant, estimated at 10^{-13} M (Akasaka et al., 1982a), cannot be determined by standard methods. Monomers have been detected only in the presence of denaturants (Inouye et al., 1979). At pH 7, SSI apparently remains dimeric as the temperature is raised until it unfolds at temperatures >80 °C and then dissociation occurs during the unfolding process (Takahashi & Sturtevant, 1981). No dissociation or unfolding is detectable in NMR spectra at 25 °C and pH <13 (Fujii et al., 1981), at 50 °C and pH <12 (Akasaka, 1978), or at pH 7 and <85 °C (Akasaka et al., 1982b,c). That is, there is no change in the ^1H NMR spectrum under these conditions. Either unfolding or dissociation of monomers without unfolding would disrupt the extensive β-sheet contacts at the interface and significantly change the magnetic environments of many protons. In addition, the only groups titrating under the conditions of these experiments are the N-terminal amino group, with pK ~ 9 at 25 °C (Akasaka, 1985), and Tyr-7, with pK = 10.6 at 50 °C (Fujii et al., 1981). The N-terminus is at the end of a six-residue stretch not observed in the X-ray data, presumably because it is highly flexible (Mitsui et al., 1981). The next residue, Tyr-7, is observed, and its phenol ring is almost fully exposed (Fujii et al., 1981). The titration of these exposed residues is not expected to affect the stability of the dimer or k_1.

In conclusion, several parameters for the cooperative unfolding transition derived from a two-process analysis of the SSI hydrogen exchange data are in reasonable agreement with other experimental data on reversible denaturation. This supports the use of the two-process scheme as a working model, according to which the upward deviation at pH >9.5 of the experimental points from the calculated curve in Figure 2 indicates the onset of a lower activation energy process, in which exchange is governed by fluctuations that are not equivalent to major unfolding.

Although only peak 1 represents a single proton, the rate constants obtained for peaks 1–5 are consistent with the two-process model in that the exchange rate constants at pH 10.5 and their activation energies are distributed over a broader range than at pH 7 or 9. However, the range of exchange rates and activation energies is smaller than in other proteins for which the low activation energy process is taken to reflect fluctuations of the folded state. In addition, the values for $\Delta H^‡$ at pH 10.5 are more than twice those typically observed for the low activation energy process in other proteins. This could indicate that the energy barriers for exchange of the core SSI protons from the folded state are considerably higher than those for buried NH's in other proteins. Alternatively, the lower activation energy process in this case may be a partial unfolding transition, possibly associated with dimer dissociation, that is not normally seen for proteins having a less extensive rigid core. In either case, the large temperature coefficients for the exchange rate constants at pH 10.5 indicate that the core of the protein is exceptionally inaccessible to solvent.

In summary, the clear division of hydrogen exchange rates into nonoverlapping distributions and the hydrogen exchange behavior of the core protons indicate that, in the folded SSI structure, >50% of the buried NH's are readily exposed to solvent, 10 are in an essentially inaccessible core, and only 8 protons are in regions of intermediate accessiblity. Taken together with the SSI crystallographic (Mitsui et al., 1979) and NMR (Akasaka, 1983) results, the hydrogen exchange data suggest that the SSI dimer is a single domain protein with unusually mobile surface segments arranged around an unusually stable β-sheet core composed of the dimer interface. The protease binding loop is located on a mobile surface segment, and it is feasible that its flexibility is functionally important. This in turn suggests the interesting possibility that the biological role of the rigid core is to maintain a collapsed structure stable enough to compensate the high degree of flexibility of the surface residues.

[2] For proteins in which the low activation energy process is assigned to motions of the folded state, the two-process model predicts that, while high activation energy rates increase with decreasing thermal stability, low activation energy rate constants are not correlated with the thermal unfolding temperature. This has been found to be the case for BPTI (Hilton et al., 1981) and lysozyme (Delepeirre et al., 1983).

ACKNOWLEDGMENTS

We thank Dr. M. Kainosho of Tokyo Metropolitan University for providing hydrogen exchange data prior to publication. For access to the NMR instruments used in these studies, we are indebted to Dr. I. Morishima, Department of Hydrocarbon Chemistry, Faculty of Engineering, Kyoto University, and to Dr. H. Watarti, National Institute of Physiological Sciences at Okazaki.

Registry No. Subtilisin, 9014-01-1; proteinase inhibitor, 37205-61-1; hydrogen, 1333-74-0.

REFERENCES

Abe, K., Kainosho, M., Inoue, T., & Akasaka, K. (1984) *Seibutsu Butsuri 24*, S266.
Akasaka, K. (1983) *J. Magn. Reson. 51*, 14–25.
Akasaka, K. (1985) *Int. J. Pept. Protein Res.* (in press).
Akasaka, K., Aoshima, H., & Hatano, H. (1975) *Biochim. Biophys. Acta 412*, 120–126.
Akasaka, K., Fujii, S., Hayashi, F., Rokushika, S., & Hatano, H. (1982a) *Biochem. Int. 5*, 637–642.
Akasaka, K., Fujii, S., & Hatano, H. (1982b) *J. Biochem. (Tokyo) 92*, 591–598.
Akasaka, K., Hatano, H., Tsuji, R., & Kainosho, M. (1982c) *Biochim. Biophys. Acta 704*, 503–508.
Akasaka, K., Hayashi, F., Hatano, H., Tonomura, B., Iwanari, H., & Hiromi, K. (1983) *Tanpakushitsu Kozo Toronkai 34*, 45–48.
Delepierre, M., Dobson, C., Selvarajah, S., Wedin, R., & Poulsen, F. (1983) *J. Mol. Biol. 168*, 687–692.
Dubs, A., Wagner, G., & Wuthrich, K. (1979) *Biochim. Biophys. Acta 577*, 177–194.
Fujii, S., Akasaka, K., & Hatano, H. (1980) *J. Biochem. (Tokyo) 88*, 789–796.
Fujii, S., Akasaka, K., & Hatano, H. (1981) *Biochemistry 20*, 518–523.
Hilton, B. D., Trudeau, K., & Woodward, C. K. (1981) *Biochemistry 20*, 4697–4703.
Hirono, S., Nakamura, E., Iitaka, Y., & Mitsui, Y. (1979) *J. Mol. Biol. 131*, 855–869.
Ikenaka, T., Odani, S., Sakai, M., Nabeshima, Y., Sato, S., & Murao, S. (1974) *J. Biochem. (Tokyo) 76*, 1191–1210.
Inouye, K., Tonomura, B., & Hiromi, K. (1979) *Arch. Biochem. Biophys. 192*, 260–269.
Komiyama, T., Miwa, M., Yatabe, T., & Ikeda, H. (1984) *J. Biochem. (Tokyo) 95*, 1569–1575.
Kossiakoff, A. A. (1982) *Nature (London) 196*, 713–721.
Lapanje, S. (1978) *Physiochemical Aspects of Protein Denaturation*, p 202, Wiley, New York.
Matsumori, S., Tonomura, B., & Hiromi, K. (1982) in *Abstracts of the Annual Meeting of the Agricultural Chemical Society of Japan*, p 355, Japan Society of Agricultural Chemistry, Tokyo.
Mitsui, Y., Satow, Y., Watanabe, Y., & Iitaka, Y. (1979) *J. Mol. Biol. 131*, 697–724.
Nakanishi, M., & Tsuboi, M. (1976) *Biochim. Biophys. Acta 434*, 365–376.
Pohl, F. M. (1968) *Eur. J. Biochem. 7*, 146–152.
Privalov, P. L., & Khechinashvili, N. N. (1974) *J. Mol. Biol. 86*, 665–684.
Sato, S., & Murao, S. (1973) *Argic. Biol. Chem. 37*, 1067–1074.
Sato, S., & Murao, S. (1974) *Agric. Biol. Chem. 38*, 587–594.
Satow, Y., Wantanabe, Y., & Mitsui, Y. (1980) *J. Biochem. (Tokyo) 88*, 1739–1755.
Segawa, S., Husimi, Y., & Wada, A. (1973) *Biopolymers 12*, 2521–2530.
Takahashi, K., & Sturetevant, J. M. (1981) *Biochemistry 20*, 6185–6190.
Takahashi, T., Nakanishi, M., & Tsuboi, M. (1978) *Bull. Chem. Soc. Jpn. 51*, 1988–1990.
Woodward, C. K., & Hilton, B. D. (1980) *Biophys. J. 32*, 561–575.
Woodward, C. K., Simon, I., & Tuchsen, E. (1982) *Mol. Cell. Biochem. 48*, 135–160.

Probable Role of Amphiphilicity in the Binding of Mastoparan to Calmodulin†

Lynda McDowell,‡ Gautam Sanyal,§ and Franklyn G. Prendergast*,‡
Departments of Pharmacology and Cell Biology, Mayo Foundation, Rochester, Minnesota 55905
Received November 15, 1984

ABSTRACT: Two-dimensional helical wheel diagrams and calculations of mean hydrophobic moments show mastoparan, mastoparan X, and *Polistes* mastoparan to have all the properties expected for amphiphilic helices. Circular dichroic properties are consistent with a random form for these peptides in dilute aqueous solution, but >50% helix is apparent when the peptides are dissolved in 70% trifluoroethanol/water mixtures (v/v) or when the peptides are bound to calmodulin. Changes in the fluorescence spectra, anisotropy, and accessibility of tryptophan whose indole side chain is on the apolar surface of the amphiphilic helix imply a significant role for the apolar surface in the binding of the mastoparans and another amphiphilic peptide, melittin, to calmodulin. These data provide a useful model for designing high-affinity synthetic peptide inhibitors of calmodulin.

Several small peptides have been found recently to bind with high affinity to calmodulin and to inhibit expression of function in this protein (Weiss et al., 1980; Malencik & Anderson, 1982, 1983a,b, 1984; Giedroc et al., 1983; Comte et al., 1983; Maulet & Cox, 1983). Melittin, a 26 amino acid peptide, and mastoparans, a group of three tetradecapeptides (see Figure 1 for sequences), have the highest affinities of the peptides studied to date. The dissociation constants for the complexes of calmodulin with mastoparan, mastoparan X, and *Polistes*

† This work was supported in part by National Institutes of Health Grant GM 31241 and by the Mayo Foundation. F.G.P. is an established investigator of the American Heart Association.
‡ Department of Pharmacology.
§ Department of Cell Biology.

0006-2960/85/0424-2979$01.50/0